Ab initio high-pressure thermodynamics of cationic disordered $MgAl_2O_4$ spinel

2003 J. Phys.: Condens. Matter 15 7103

(http://iopscience.iop.org/0953-8984/15/41/018)

INSTITUTE OF PHYSICS PUBLISHING JOURNAL OF PHYSICS: CONDENSED MATTER

J. Phys.: Condens. Matter **15** (2003) 7103–7115 PII: S0953-8984(03)65035-6

Ab initio high-pressure thermodynamics of cationic disordered $MgAl_2O_4$ spinel

S Da Rocha[1,2] **and P Thibaudeau**[1]

[1] Commissariat à l'Energie Atomique, Le Ripault, BP 16, F-37260 Monts, France
[2] Laboratoire d'Electrodynamique des Matériaux Avancés, UMR 6157 CNRS CEA, Faculté des Sciences et Techniques, Université François Rabelais, Parc de Grandmont, F-37000 Tours, France

E-mail: pascal.thibaudeau@cea.fr

Received 17 June 2003
Published 3 October 2003
Online at stacks.iop.org/JPhysCM/15/7103

Abstract

Ab initio calculations are performed in the framework of density functional theory and the local density approximation, to evaluate structural, thermodynamic and vibrational behaviour of $MgAl_2O_4$ spinel with cationic disorder under pressure. An effective thermodynamic model using both a regular solution and a quadratic form for the internal energy is parametrized to describe the non-convergent cationic disordering. The evolution of cationic disorder rate with temperature and isostatic pressure is deduced from this model. Relative density and heat capacity excess evolution are simulated as a function of cationic disorder. Infrared modes are calculated in the Brillouin zone centre for several disordered spinels. Good agreement is found with available experimental data.

1. Introduction

Spinels belong to the ceramic oxide family and have a wide range of applications in geophysics [1], magnetism [2] and irradiated environments [3, 4]. The general formula of a II–III spinel is AB_2O_4, where A is a divalent cation (such as Mg^{2+}, Zn^{2+}, Cd^{2+} etc) and B a trivalent cation (such as Al^{3+}, Ga^{3+}, In^{3+} etc). Among the spinel family, $MgAl_2O_4$ is often considered as a model of spinel structure where the oxygen atoms form a close-packed pseudo face-centred cubic sublattice. Among all the 96 possible interstices of the anions lattice, 64 are tetrahedral (IV) and 32 are octahedral (VI). In a so-called normal arrangement, one tetrahedral site in eight is occupied by divalent cations, whereas trivalent cations occupy half of the octahedral sites [5]. Barth and Posnjak [6] have outlined that the normal arrangement cannot reproduce the intensity of x-ray diffraction pattern of some spinels. So, they have suggested an arrangement where equivalent positions are occupied by different atoms according to the following general formula: $B^{IV}(AB)^{VI}O_4$. However, it is now well known that spinels can

accommodate cationic disorder [7, 8]. An inversion parameter, usually labelled x, has been introduced to quantify the number of trivalent B ions (in the present work Al^{3+}) located in tetrahedral interstices.

The $MgAl_2O_4$ spinel can then be described by the following formula:

$$(Mg_{(1-x)}Al_x)^{IV}[Mg_xAl_{(2-x)}]^{VI}O_4,$$

where x ranges from 0 (normal spinel) to 1 (fully inverse spinel). It has been shown that cationic disorder is activated by either pressure [9] or particle irradiations such as neutrons, electrons or Ne^+ ions [10, 11]. However, the usual and probably easiest way to activate disorder by cationic exchange, in both natural and synthetic spinel, is to heat the studied specimen [12]. Successive heat pulses can also be applied to samples to synthesize directly disordered spinels [13].

It is now commonly admitted that most of the spinels belong to the $Fd\bar{3}m$ (227) space group. However, the experimental observations reported by many groups [14–16, 13, 17] suggest a lower-symmetry space group for some of these structures. In particular, Schmocker and Waldner [13] have outlined that, in an inverse spinel, domains of reduced symmetry are responsible for observed extra Bragg reflections. This suggests a possible connection between the inversion parameter x and the space group of the structure, whereas Haas [18] has claimed that cation disorder does not induce natural change in structure symmetry.

Up to now, most of the reported experimental studies on spinels deal with the determination of x with respect to temperature. Electron spin resonance (ESR) on a natural $MgAl_2O_4$ spinel for temperatures lower than 1278 K [7] and high-resolution ^{27}Al nuclear magnetic resonance (NMR) on quenched natural or synthetic samples [19–21] have been intensively developed to investigate such behaviour. Several other techniques have been reported such as Raman spectroscopy [22], neutron diffraction [23, 24], which both allow *in situ* measurements, and x-ray diffraction [25, 26]. Because of various experimental techniques and sample preparations, discrepancies appear in the reported data.

To complete structural analysis and avoid experimental difficulties, some theoretical investigations have been carried out to study the disorder effect on spinel stability. Wei and Zhang [27] have selected 18 members among II–III and IV–II spinels to evaluate the most stable form between normal and inverse configurations. They have also calculated, at *ab initio* level, structural parameters such as the lattice constant, the average internal oxygen position and bandgaps in both configurations. Most of these spinels are found to be stable in normal structure except for $MgGa_2O_4$ and $MgIn_2O_4$ in the II–III family and $GeMg_2O_4$ and all Si spinels in the IV–II group. Moreover, bandgaps are found to be smaller in the inverse configuration. To explore cationic disorder continuous variations, Warren *et al* [28, 29] have investigated disordered spinel thermodynamic properties with temperature. In their approach, short-range one-site cluster potentials have been parametrized from a small number of disordered configurations within density functional theory (DFT) in both the local density approximation (LDA) and the general gradient approximation (GGA). These potentials have been applied in Monte Carlo simulations to predict disordering thermodynamics state variables.

Alternatively, the volume thermal expansion and specific heat of alumina–magnesium systems with temperature have been evaluated using both molecular dynamics and experimentally derived interatomic potentials [30]. In spite of a well reproduced heat capacity curve, the predicted thermal expansion appears to be significantly lower at high temperature than experimentally observed.

Most of the experimental and theoretical investigations reported in the literature were performed on spinel cations behaviour with temperature and normal pressure. High-pressure spinel phases have been studied at *ab initio* level [31, 32] but connection between these phases and the observed normal-pressure cubic-like disordered form was never clearly established.

Thus, to our knowledge, it seems that no complete study has been previously carried out to evaluate the variation of both structural and thermodynamical spinel properties with cationic disorder under high pressure.

In this study, *ab initio* calculations have been performed to evaluate, firstly, the influence of cationic disorder on internal energy variation and excess of heat capacity evolution, and secondly the relative density behaviour under pressure. For several pressures, the cationic disorder parameter as a function of temperature curve is deduced as a by-product, according to a modified effective thermodynamic model using both a regular solution and a quadratic form of the internal energy [33]. Infrared phonons are calculated using density functional perturbation theory (DFPT) for selected disordered spinels to investigate cationic disorder experimental evidence in IR spectra. Results are compared with available experimental data.

2. Calculation methodology

To approximate the continuous variation of x, 56-atom cubic supercells are generated. Starting from the normal cation distribution, N Mg and Al atoms are randomly switched among all the cations, with N ranging from zero to eight, such that the dimensionless inversion parameter x is defined as $N/8$. Because it is computer time demanding, only five different supercells for each cationic arrangement are selected to average cell energy and structural behaviour of the disordered crystal.

Simulations are performed using the ABINIT[3] code within DFT and LDA to calculate the total electronic energy, the forces acting on atoms and the cell stress. The valence electrons are described by pseudopotentials developed on a plane waves basis set. The generation of the cation pseudopotentials follows the scheme proposed by Hamann [34], whereas the oxygen follows the Troullier–Martins scheme [35]. The particular choice of these pseudopotential schemes is detailed elsewhere [36]. During calculations, symmetries are turned off to keep the P_1 space group.

To integrate into the whole Brillouin zone, a k-point sampling is required. In previous studies, Warren *et al* [28] have chosen a finite $2 \times 2 \times 2$ Monkhorst–Pack set of irreducible k-points for all the configurations. In normal spinel a sufficient large centred or shifted grid should be used because of the symmetries. However, to reduce the computer time demand, a mandatory small set of k-points is required for all the DFT calculations. The disordered configurations could be calculated with such a grid but each disordered cell has to be treated with the same closest numerical accuracy. However, the variation of geometry induced by disorder changes deeply the generation of an optimum k-point grid, thus a compromise solution must be found.

The band structure of the normal $MgAl_2O_4$ spinel has been calculated by Xu and Ching [37] using the orthogonalized linear combination of atomic orbitals method in LDA. For the higher-energy valence bands, a gap was found at the zone centre which is partially filled taking into account all the points in the Brillouin zone as shown in their electronic density of states. So in the case of a non-disordered spinel, because of the symmetries, keeping the zone centre only is a partial approximation. However, Mo and Ching [38] have shown in disordered spinel that, for the same bands, no gap structure remains in the electronic density of states. This suggests a possible level degeneracy shift by an increase of cationic disorder. In that case, keeping only the Γ point in DFT calculations becomes again a well founded approximation. Finally, as the supercell volume is large and the wavefunction symmetry reductions have been turned off,

[3] The ABINIT code is a common project of the Université Catholique de Louvain, Corning Incorporated, Université de Liège, CEA, Mitsubishi Chemical Corp. and other contributors (URL http://www.pcpm.ac.be/abinit).

the zone centre point is kept as an approximation during all the calculations. Nevertheless, to neglect induced modifications of the Brillouin zone shape, the maximum pressure is monitored to keep a cell parameter reduction that never exceeds 1% of the normal spinel equilibrium volume.

For each disorder rate and each configuration, cell vectors and atomic positions are relaxed after several self-consistent cycles using conjugate gradient techniques. The simulation stops when all the forces and resulting stresses are close to a desired numerical precision.

As DFT calculations are performed to zero temperature, an effective thermodynamic model, first introduced by Néel [39] and popularized by O'Neill and Navrotsky [33], is required to determine the equilibrium inversion parameter for a given temperature and pressure. The main quantity in this model is the Gibbs free enthalpy excess induced by disorder, labelled ΔG, which usually includes a quadratic internal energy with the disorder rate ΔU, a specific form of configuration entropy ΔS_c and a work of external pressure P (through $P\Delta V$) such as

$$\Delta G = \Delta U - T\Delta S_c + P\Delta V. \tag{1}$$

When calculations are carried out without external pressure, no extra work induced by pressure forces is necessary to keep a constant energy. Then, one has

$$\Delta U = \alpha x + \beta x^2, \tag{2}$$

$$\Delta S_c = -k_B\left[x\ln x + (1-x)\ln(1-x) + x\ln\frac{x}{2} + (2-x)\ln\left(1-\frac{x}{2}\right)\right], \tag{3}$$

where k_B is the Boltzmann constant. In this case, the Gibbs free enthalpy is reduced to the Helmholz free energy introduced by O'Neill and Navrotsky as expected.

The α and β constants are deduced from our *ab initio* calculations. From a physical point of view, they are linked to both the chemical potential, which states that this system has two kinds of inequivalent cationic occupied site, and an exchange energy value, which is partially non-linear with the disorder rate.

For a given set of temperature and pressure, once ΔG is established, the extremum condition

$$\frac{\partial \Delta G}{\partial x(P,T)} = 0 \tag{4}$$

is numerically solved to determine the average equilibrium cationic distribution. In addition, using this derived $x(P, T)$ equilibrium curve and the configurational entropy, the heat capacity excess induced by disorder is calculated according to the following equation for several pressures:

$$\Delta C_p(T) = \left(\frac{\partial \Delta H}{\partial T}\right) = T\left(\frac{\partial \Delta S_c}{\partial T}\right)_P. \tag{5}$$

To complete the description, it has been observed both experimentally [26] and in our simulations that the spinel cell volume varies with the disorder. To reproduce this behaviour, the induced volume modification is approximated by a quadratic expression with x (equation (6)), where μ and ν are coefficients also deduced from *ab initio* calculations,

$$\Delta V = \mu x + \nu x^2. \tag{6}$$

Then, it is convenient to introduce two effective parameters α' and β' (equations (7) and (8)) to mimic the model previously considered by O'Neill and Navrotsky. These effective constants are found to behave linearly with pressure

$$\alpha' = \alpha + P\mu, \tag{7}$$

$$\beta' = \beta + P\nu. \tag{8}$$

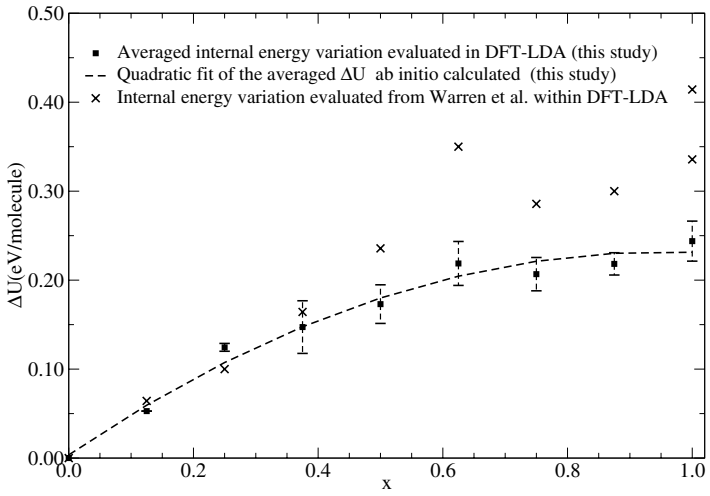

Figure 1. Average internal energy variation with cationic disorder calculated within LDA (□) and compared to LDA results from Warren *et al* (×) [28].

Table 1. Comparison of experimental and *ab initio* calculated α and β parameters (eV/molecule) and mean-squared errors.

	References	α	$\Delta\alpha$	β	$\Delta\beta$	Method
Theory	This work	0.48	0.08	−0.25	0.06	DFT-LDA
	[28]	0.60	—	−0.22	—	DFT-LDA
Exp.	[20]	0.26	0.06	0.06	0.10	RMN ^{27}Al
	[21]	0.36	0.06	−0.33	0.06	RMN ^{27}Al
	[23]	0.32	0.01	−0.10	0.03	Neutron diffraction
	[24]	0.34	0.01	0.05	0.02	Neutron diffraction
	[26]	0.24	0.02	0.14	0.05	X-ray diffraction

3. Results and discussion

3.1. Calculations without external applied pressure

3.1.1. Variation of internal energy. As shown in figure 1, the average energy difference $\Delta U(x) = U(x) - U(0)$ is calculated and compared with results from Warren *et al* [28]. Discrepancies between the two sets of calculations could have their origin in different spannings of the configurational space. Mean-squared error on ΔU clearly shows that a single calculation per inversion parameter is not sufficient to take into account the configurational space variety. As the internal energy differences are small, the absolute criteria of force convergence on atoms (up to 10^{-4}) and the resulting stress on the cell (up to 10^{-8}) have been carefully monitored during the calculations. A quadratic fit of ΔU provides both average α and β values and $\Delta\alpha$ and $\Delta\beta$ errors. These values are reported and compared with available experimental data in table 1. Larger differences have been reported on β than α. In their analysis of cationic distribution, O'Neill and Navrotsky [33] have shown that α and β should be approximately of equal magnitude and opposite sign.The proposed reason for this sign difference was induced by the ionic character of the bindings in spinels. As shown by Thibaudeau and Gervais [36] in normal spinel, the Born effective charges on atoms are very close to the full ionic charges.

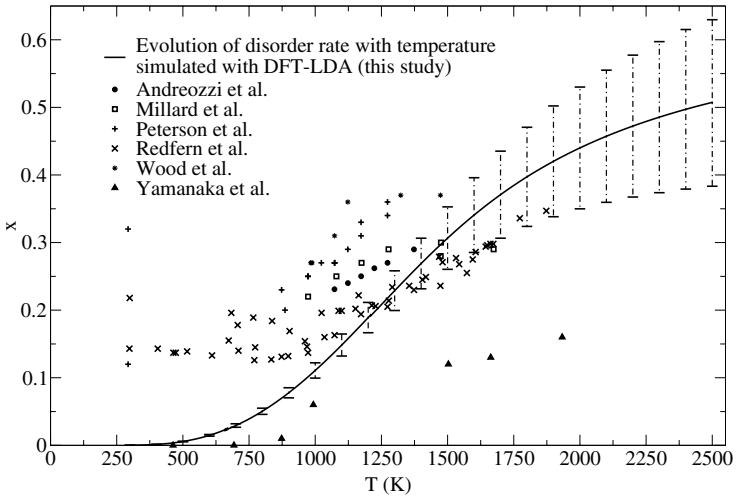

Figure 2. Disorder rate x obtained solving equation (4) and compared to neutron scattering experiments [24] (×), [23] (+), x-ray measurements [25] (△), [26] (●) and ^{27}Al NMR experiments [20] (□), [19] (∗).

So, at least for low disorder rate, the ionic character should be preserved when cations switch. As shown in table 1, this study and some of the reported data [28, 21, 23] fulfil the opposite sign criterion and could be considered from this point of view as most reliable.

3.1.2. Disorder equilibrium curve and heat capacity. Variations of the disorder rate with temperature are deduced from the extremum condition on the Gibbs free enthalpy. The derived curve is compared to most of the available experimental data in figure 2. This figure shows that significant differences between internal energy parameters are not sufficient to predict accurate variations of x in a function of temperature. This curve also shows that the uncertainties $\Delta\alpha$ and $\Delta\beta$ can give an insight into conclusions between different experimental and theoretical works. Because the experimental extent of temperatures is limited, an accurate determination of the internal energy variation appears to be more difficult for the quadratic coefficient β than for α. To quantify β more accurately, experimental investigation should increase the range of temperatures to higher values.

In spinels, several thermodynamic observables exhibit rapid variations with temperature which suggest a possible second-order phase transition. A discontinuity in cell edge and thermal expansion coefficient has been observed by several groups [25, 40], but Kashii *et al* [41] using the NMR technique have reported, on the basis of kinetic considerations, that the cationic equilibrium disorder reaction is a first-order transition. In this study, the second-derivative calculation of the free energy ΔG with respect to the temperature was performed for several pressures. Once the equilibrium variation of x as a function of temperature is known, the determination of configurational entropy and its first derivative with temperature drop naturally according to equation (5). As shown in figure 3, ΔC_p exhibits a peak which is typical of a continuous phase transition. The harmonic part of heat capacity at constant pressure is by far the main contribution to the total capacity in spinels [30]. However, the increase at maximum of heat capacity induced by disorder for zero pressure is about 15 J mol^{-1} K^{-1} and should be experimentally observed. This maximum value suggests a critical temperature definition for this system. However, another critical temperature is usually introduced to describe order–disorder transitions [42]. Its determination is strongly connected to the Bragg–Williams model

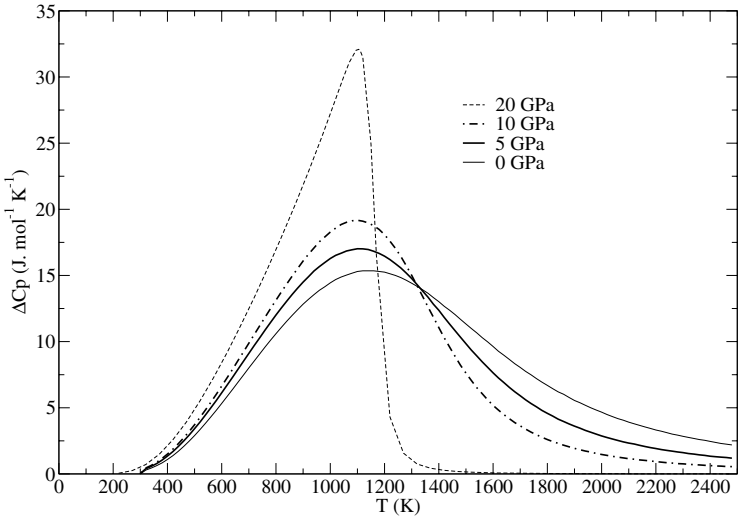

Figure 3. Heat capacity induced by disorder curves as a function of temperature and pressure.

for metals. In this model, the solution of

$$\left(\frac{\partial^2 \Delta G}{\partial Q^2}\right)_{Q=0,T=T_c} = 0, \tag{9}$$

where Q is an order parameter, gives the required temperature T_c. In the case of II–III spinels, it is possible to define an order parameter $Q = 1 - (3/2)x$ connected to the cationic occupation, which varies from unity (maximum order) to zero (random disorder). Solving equation 9, with the Gibbs free energy form introduced previously, gives $T_c = -8\beta'/27k_B$, where k_B stands for the Boltzmann constant. Using our derived *ab initio* values, $T_c \approx 860$ K when $P = 0$. This temperature is in fair agreement with the previously reported experimental values of 870 K $\leqslant T_c \leqslant$ 970 K [25], $T_c \approx 950$ K [43] and $T_c \approx 930$ K [40]. As T_c is defined positive, the sign of β is expected to be negative or zero.

3.1.3. Density as a function of disorder behaviour. Discrepancies have been reported in the density behaviour with the cationic disorder. The determination of volume variation induced by the disorder is only a difficult task on quenched samples. Wood *et al* [19] have carried out ^{27}Al NMR experiments on quenched synthetic spinels and found a cell volume increase of 0.03% for an increase of x from 0.21 to 0.39. An x-ray study performed on a quenched single crystal has shown a decrease in cell parameters with increasing disorder [25]. Using a description based on ionic radii, O'Neill and Navrotsky [33] have predicted a decrease in volume with disorder for all the II–III spinels with cations of similar size to Mg^{2+} and Fe^{3+}. *Ab initio* calculations performed in this study agree to a density increase with cationic exchange. They are compared with recent x-ray measurements on quenched single crystals reported by Andreozzi and co-workers [26] in figure 4. Conclusive agreement is found at least for the range of temperature experimentally observed by this group.

3.2. External pressure effects

To investigate pressure effects on cationic disorder, calculations are performed for 5, 10 and 20 GPa. A target stress is imposed during simulation on the same five generated configurations

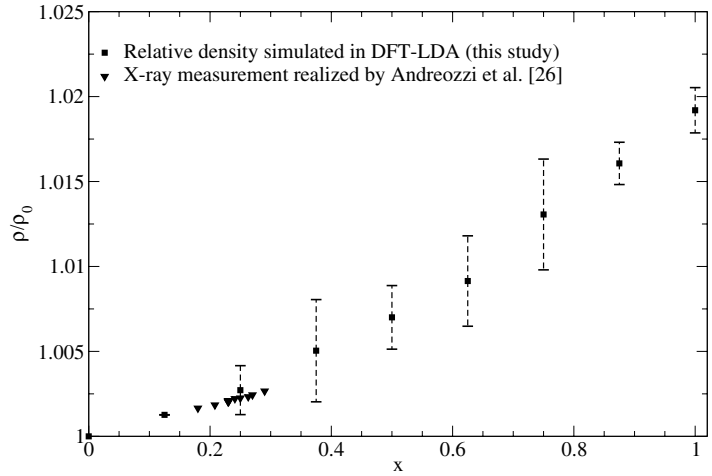

Figure 4. Relative density behaviour with x *ab initio* calculated (□) and compared with x-ray measurements (△) [26].

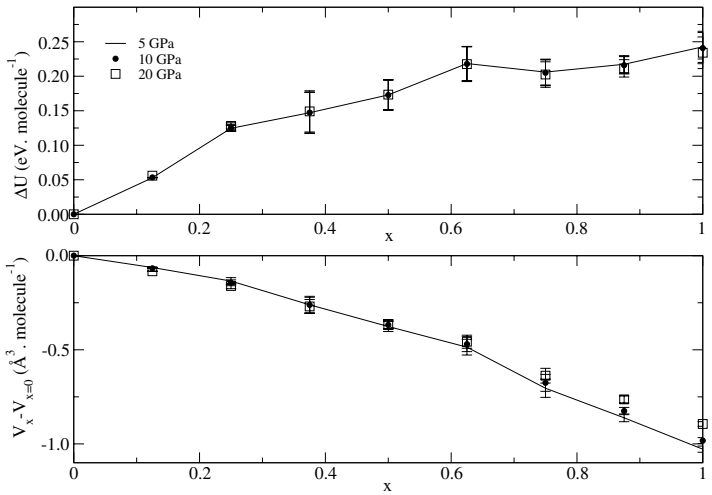

Figure 5. Variation of ΔU and ΔV as a function of disorder rate x for 5, 10 and 20 GPa.

per disorder rate. Average variations ΔU and $\Delta V(x) = V(x) - V(0)$ are evaluated for these pressures. Figure 5 shows the evolution of internal energy and volume differences for 5, 10 and 20 GPa. Few changes appear. α, β, μ and ν parameters deduced are collected in table 2. Figure 6 reports a decrease of α' and β' with increasing pressure. These curves show that, at least for disorder up to 0.6, the internal energy difference is not affected by the pressure. So the bindings in disordered spinels appear to be unaffected when a moderate pressure is applied. However, for highly disordered spinels, the cell volume shrinks more rapidly when the pressure is low. This could be explained by cation steric packing which is higher with pressure. Figure 7 collects the equilibrium disorder rate obtained for 5, 10 and 20 GPa. The zero-pressure case is reported for the record. Variations in x induced by pressure have different magnitudes according to the temperature considered. For temperature lower than 1000 K pressure effects

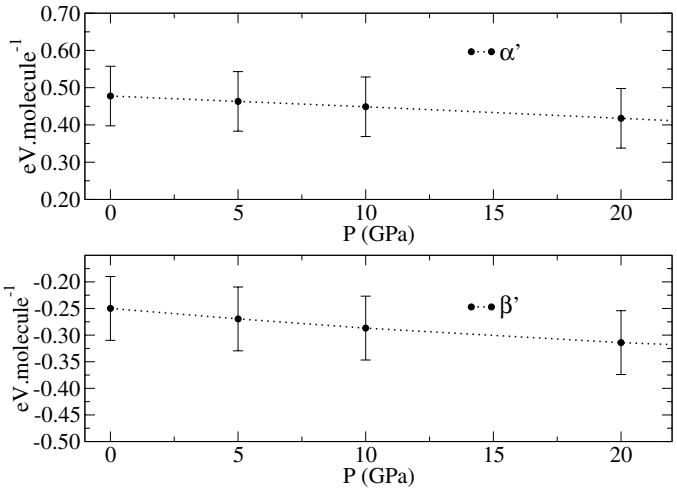

Figure 6. Variation of α' and β' with pressure in GPa. A straight line is drawn for 5 GPa and helps as a guide for the eyes.

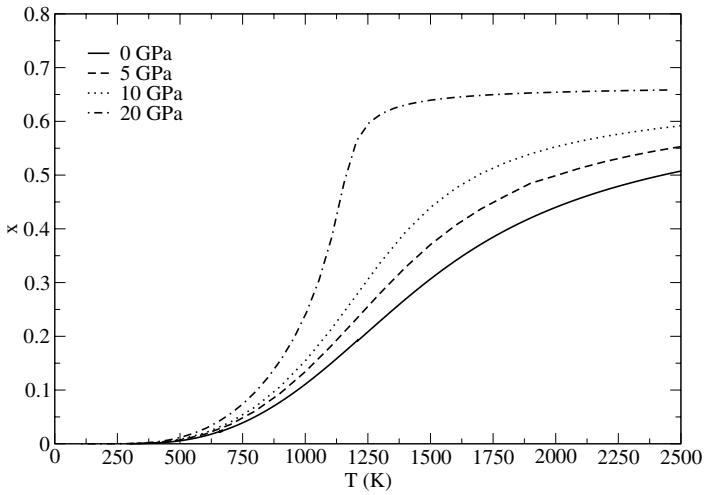

Figure 7. Equilibrium $x = f(T)$ curves for several pressures up to 20 GPa. The zero-pressure curve was redrawn for clarity.

on x are negligible, while for high temperature effects are more substantial. For 20 GPa and temperature up to 1400 K, x quickly reaches the maximum value, $\approx 2/3$, allowed. This could be a possible explanation for the disproportionation observed many years ago by Liu [44]. Liu observed that the strongest x-ray diffraction lines for a heated and compressed spinel sample could be produced by a mixture of periclase and corundum. He also deduced that the short-range ordering of the spinel gradually disappeared with increasing pressure and temperature. According to Liu, the spinel x-ray short-range order vanished at 1300–1700 K and 20 GPa. These values are in complete agreement as shown in figure 7, where the spinel is maximally disordered in these regimes. The relative stability of an oxide mixture over the spinel was also predicted by Catti [32] using *ab initio* techniques, supporting a short-range vanishing spinel

Table 2. *Ab initio* calculated α, β, μ and ν parameters for different pressures: errors on α, β, μ and ν are respectively ± 0.08, ± 0.06, ± 0.2 and ± 0.08 for all pressures.

Pressure	α	β	μ	ν	α'	β'
(GPa)	(eV/molecule)		(Å^3/molecule)		(eV/molecule)	
0	0.48	−0.25	−0.54	−0.63	0.48	−0.25
5	0.48	−0.25	−0.47	−0.58	0.46	−0.27
10	0.48	−0.25	−0.48	−0.51	0.45	−0.29
20	0.49	−0.27	−0.56	−0.34	0.42	−0.31

structure with pressure. However, the expected division of spinel into a mixture of its oxides is rather incompatible with the restructuring of a single crystal on pressure release recently found by Wittlinger and co-workers [45]. On the other hand, the restructuring is fully compatible with a cationic equilibrium curve as found in the present work.

4. Infrared vibrational spectra of disordered spinel

Maradudin and co-workers [46] have demonstrated that the macroscopic low-frequency static dielectric permittivity tensor $\epsilon_{ij}(\omega)$ which gives the infrared spectra main contribution is the sum of both an ionic part and a limit value of a pure electronic contribution. Following Gonze and Lee [47], one has

$$\epsilon_{ij}(\omega) = \epsilon_{ij}^{\infty} + \frac{4\pi}{\Omega_0} \sum_m \frac{\left(\sum_{\kappa i'} Z^*_{\kappa,ii'} U^*_{m,\mathbf{q}=\mathbf{0}}(\kappa i')\right)\left(\sum_{\kappa' j'} Z^*_{\kappa',jj'} U_{m,\mathbf{q}=\mathbf{0}}(\kappa' j')\right)}{\omega_m^2 - \omega^2} \tag{10}$$

where $1 \leqslant i, j \leqslant 3$, Ω_0 is the cell volume, $Z_{\kappa,ii'}$ are the Born effective tensors and ϵ_{ij}^{∞} is the electronic contribution to the dielectric permittivity tensor. This last tensor is given by the knowledge of the second derivative of the total electronic energy with the macroscopic electric field. Here $\{\omega_m^2\}$ represent the dynamical matrix eigenvalues and $\{U_{m\mathbf{q}}\}$ the corresponding eigenvectors of the mode m with the following normalization:

$$\sum_{\kappa j} M_k [U_{m\mathbf{q}}(\kappa j)]^* U_{n\mathbf{q}}(\kappa j) = \delta_{mn}, \tag{11}$$

where M_k are the atomic masses.

Powerful techniques were developed a few years ago to calculate vibrational properties of extended systems through DFPT [48]. This technique has been applied successfully to evaluate all vibrational modes at the zone centre for normal cubic $MgAl_2O_4$ spinel [36]. The Born effective charges have also been evaluated within DFPT and compared to a set of new experiments on synthetic spinels [36]. The agreement was found satisfactory, demonstrating that the ionic character was preserved in this spinel even on a synthetic and probably low-disorder compound.

Many groups have reported extra infrared modes for synthetic $MgAl_2O_4$ spinels [49, 36] and highly non-symmetric peaks in the Raman spectra for quenched samples [50]. The precise origin of these extra modes is unclear [49] but an extra Raman mode near 727 cm^{-1} was clearly assigned to the symmetric Al–O stretching vibration of AlO_4 groups created by the redistribution of some aluminium ions from octahedral to tetrahedral sites. However, to explore the possibility that infrared modes originate from cationic disorder, dynamical matrix eigenvectors and eigenvalues have been calculated within DFPT for several inversion parameters and averaged on different configurations. The imaginary parts of the low-frequency dielectric tensor components are reported in figure 8. A lifetime mode is required for

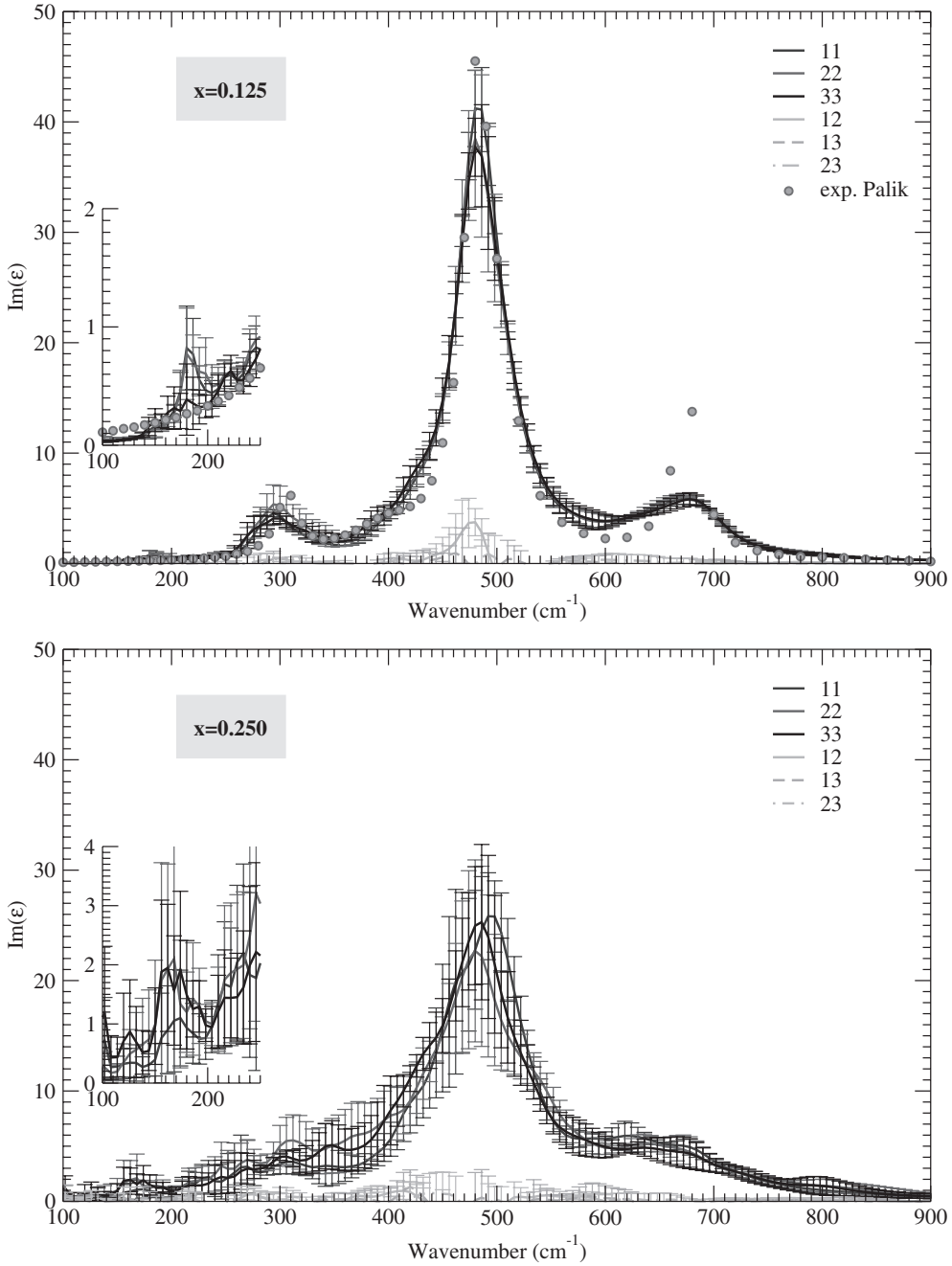

Figure 8. Behaviour of all six independent components of the imaginary part of the dielectric tensor in the IR regime for several disorder rates. Experiments are taken from [52].

each state such that its corresponding damping over its frequency is a constant for a given temperature [51]. As room temperature is high enough to neglect the anharmonic residual quantum effect for low temperatures, assuming a linear behaviour of damping with temperature

is a natural approximation. It is important to keep in mind that constant interactions of different phonons is a crude approximation. However, following this hypothesis, examination of both experimental LO and TO dampings and frequencies measured for two sets of synthetic spinels provides a linear regression coefficient of 80%. This value is high enough to consider the ratio between damping and frequency as a constant. The corresponding value of this constant was fitted using previously measured damping and frequencies [36]. For simplicity, anharmonicity is assumed to be sufficiently small for low inversion parameter such that this constant remains unchanged. Using these approximations, the intensity of all the T_{1u} normal spinel infrared modes decreases when the inversion parameter increases as shown in figure 8. Experimental measurements published by Tropf and Thomas [52] were reported in the first part of figure 8. A disorder of $x = 0.125$ was assumed for experimental data in order to compare with our calculated spectra. This value was experimentally observed for synthetic cooled spinels [24] at room temperature. As shown in these figures, when the disorder increases the resulting widths become larger and several modes near 800 and 180 cm^{-1} become intense. These extra modes have been previously observed [36] in different synthetic spinels and then could have their origin in the defective nature of the spinel lattice.

5. Conclusion

Structural and thermodynamic properties of disordered $MgAl_2O_4$ spinel were calculated by DFT with a plane-wave basis set and pseudopotentials. Several configurations were considered to average each property to take account of configurational variety. The evolution of internal energy was calculated as a function of cationic disorder rate. Variations of disorder rate with temperature and pressure were determined using a completed effective thermodynamic model. By taking into account the mean-squared errors obtained on α and β parameters, an original approach of the cationic equilibrium curve was introduced. Furthermore, the excess of heat capacity exhibits a typical behaviour which is the sign of a continuous transition. A critical temperature as a function of the pressure is also evaluated for a perfect random crystal. A possible explanation for the previously reported disproportionation was given. In addition, it has been shown that $MgAl_2O_4$ spinel density increases with increasing disorder. Finally, infrared spectrum calculations of selected inversion parameters were carried out within DFPT and have shown extra modes which could originate in this particular defective nature of the spinel lattice.

References

[1] Lucchesi S and Della Giusta A 1997 *Mineral. Petrol.* **59** 91–9
[2] Schiessl W, Poltzel W, Karzel H, Steiner M and Kalvius G M 1996 *Phys. Rev.* B **53** 9143–52
[3] Yu N, Sickafus K E and Nastasi M 1994 *Phil. Mag. Lett.* **70** 235–40
[4] Zinkle S J 1995 *J. Nucl. Mater.* **219** 113–27
[5] Sickafus K E and Wills J M 1999 *J. Am. Ceram. Soc.* **82** 3279–92
[6] Barth T F W and Posnjak E 1932 *Z. Kristallogr.* **82** 325–41
[7] Schmocker U, Boesh H R and Waldner F 1972 *Phys. Lett.* A **40** 237–8
[8] Hafner S and Laves F 1961 *Z. Kristallogr.* **115** 321–30
[9] Hazen R M and Navrotsky A 1996 *Am. Mineral.* **81** 1021–35
[10] Sickafus K E, Larson A C, Yu N, Nastasi M, Hollenberg G W, Garner F A and Bradt R C 1995 *J. Nucl. Mater.* **219** 128–34
[11] Soeda T, Matsumura S, Kinoshita C and Zaluzec N J 2000 *J. Nucl. Mater.* **283–287** 952–6
[12] Gorter E W 1954 *Philips Res. Rep.* **9** 403–43
[13] Schmocker U and Waldner F 1976 *J. Phys. C: Solid State Phys.* **9** L235–7
[14] Grimes N W, O'Connor P J and Thompson P 1978 *J. Phys. C: Solid State Phys.* **11** L505–7

[15] Grimes N W, Thompson P and Kay H F 1983 *Proc. R. Soc.* A **386** 333–45
[16] Hwang L, Heuer A H and Mitchell T E 1973 *Phil. Mag.* **28** 241–3
[17] Thompson P and Grimes N 1977 *J. Appl. Crystallogr.* **10** 369–71
[18] Haas C 1965 *J. Phys. Chem. Solids* **26** 1225–32
[19] Wood B J, Kirkpatrick R J and Montez B 1986 *Am. Mineral.* **71** 999–1006
[20] Millard R L, Peterson R C and Hunter B K 1992 *Am. Mineral.* **77** 42–52
[21] Maekawa H, Kato S, Kawamura K and Yokokawa T 1997 *Am. Mineral.* **82** 1125–32
[22] Cynn H, Anderson O L and Nicol M 1993 *Pure Appl. Geophys.* **141** 415–44
[23] Peterson R C, Lager G A and Hitterman R L 1991 *Am. Mineral.* **76** 1455–8
[24] Redfern S A T, Harrison R J, O'Neill H St C and Wood D R R 1999 *Am. Mineral.* **84** 299–310
[25] Yamanaka T and Takeuchi Y 1983 *Kristallographie* **165** 65–78
[26] Andreozzi G B, Princivalle F, Skogby H and Della Giusta A 2000 *Am. Mineral.* **85** 1164–71
[27] Wei S H and Zhang S B 2001 *Phys. Rev.* B **63** 045112-1–8
[28] Warren M C, Dove M T and Redfern S A T 2000 *J. Phys.: Condens. Matter* **12** L43–8
[29] Warren M C, Dove M T and Redfern S A T 2000 *Min. Mag.* **64** 311–7
[30] Morooka S, Zhang S, Nishikawa T and Awaji H 1999 *J. Ceram. Soc. Japan* **107** 1225–8
[31] Gracia L, Beltran A, Andrés J, Franco R and Recio J M 2002 *Phys. Rev.* B **66** 224114
[32] Catti M 2001 *Phys. Chem. Minerals* **28** 729–36
[33] O'Neill H St C and Navrotsky A 1983 *Am. Mineral.* **68** 181–94
[34] Hamann D R 1989 *Phys. Rev.* B **40** 2980
[35] Troullier N and Martins J L 1991 *Phys. Rev.* B **43** 1993–2006
[36] Thibaudeau P and Gervais F 2002 *J. Phys.: Condens. Matter* **14** 3543–52
[37] Xu Y N and Ching W Y 1991 *Phys. Rev.* B **43** 4461
[38] Mo S D and Ching W Y 1996 *Phys. Rev.* B **54** 16555–61
[39] Néel L 1950 *C. R. Acad. Sci. Paris* **230** 190
[40] Suzuki I and Kumazawa M 1980 *Phys. Chem. Minerals* **5** 279–84
[41] Kashii N, Maekawa H and Hinatsu Y 1999 *J. Am. Ceram. Soc.* **82** 1844–8
[42] Redfern S A T 2000 *Transformation Processes in Minerals* vol 39, ed S A T Redfern and M A Carpenter (Washington, DC: Mineralogical Society of America) pp 105–33
[43] Weeks R A and Sonder E 1979 *J. Am. Ceram. Soc.* **63** 92–5
[44] Liu L G 1975 *Geophys. Res. Lett.* **2** 9–11
[45] Wittlinger J, Werner S and Schulz H 1998 *Acta Crystallogr.* B **54** 714–21
[46] Maradudin A A, Montroll E W, Weiss G H and Ipatova I P 1971 *Solid State Physics: Advances in Research and Applications* vol 4 (New York: Academic)
[47] Gonze X and Lee C 1997 *Phys. Rev.* B **55** 10355–68
[48] Baroni S, Giannozzi P and Testa A 1987 *Phys. Rev. Lett.* **58** 1861
[49] Chopelas A and Hofmeister A M 1991 *Phys. Chem. Minerals* **18** 279–93
[50] Cynn H, Sharma S K, Cooney T F and Nicol M 1992 *Phys. Rev.* B **45** 500–2
[51] Srivastava G P 1990 *The Physics of Phonons* (Bristol: Adam Hilger)
[52] Tropf W J and Thomas M E 1991 *Handbook of Optical Constants in Solids* vol 2, ed E D Palik (New York: Academic)